ARL-TR-10124 ● JULY 2025

Additional Validation of Physics-Informed Transfer Learning for Out-of-Sample Vapor Pressure Prediction: Organic Nitrate Esters

by Michael J. McQuaid, Joshua L. Lansford, and Christopher P. Stone

DISTRIBUTION STATEMENT A. Approved for public release: distribution unlimited.

NOTICES

Disclaimers

The findings in this report are not to be construed as an official Department of the Army position unless so designated by other authorized documents.

Citation of manufacturer's or trade names does not constitute an official endorsement or approval of the use thereof.

Destroy this report when it is no longer needed. Do not return it to the originator.

ARL-TR-10124 ● JULY 2025

Additional Validation of Physics-Informed Transfer Learning for Out-of-Sample Vapor Pressure Prediction: Organic Nitrate Esters

Michael J. McQuaid, Joshua L. Lansford, and Christopher P. Stone
DEVCOM Army Research Laboratory

DISTRIBUTION STATEMENT A. Approved for public release: distribution unlimited.

REPORT DOCUMENTATION PAGE

1. REPORT DATE	2. REPORT TYPE	3. DATES COVERED	
		START DATE	END DATE
July 2025	Technical Report	October 2024	February 2025

4. TITLE AND SUBTITLE
Additional Validation of Physics-Informed Transfer Learning for Out-of-Sample Vapor Pressure Prediction: Organic Nitrate Esters

5a. CONTRACT NUMBER	5b. GRANT NUMBER	5c. PROGRAM ELEMENT NUMBER
5d. PROJECT NUMBER	**5e. TASK NUMBER**	**5f. WORK UNIT NUMBER**

6. AUTHOR(S)
Michael J. McQuaid, Joshua L. Lansford, and Christopher P. Stone

7. PERFORMING ORGANIZATION NAME(S) AND ADDRESS(ES)
DEVCOM Army Research Laboratory
ATTN: FCDD-RLA-WC
Aberdeen Proving Ground, MD 21005

8. PERFORMING ORGANIZATION REPORT NUMBER
ARL-TR-10124

9. SPONSORING/MONITORING AGENCY NAME(S) AND ADDRESS(ES)	10. SPONSOR/MONITOR'S ACRONYM(S)	11. SPONSOR/MONITOR'S REPORT NUMBER(S)

12. DISTRIBUTION/AVAILABILITY STATEMENT
DISTRIBUTION STATEMENT A. Approved for public release: distribution unlimited.

13. SUPPLEMENTARY NOTES
ORCID: Christopher P. Stone, 0000-0002-9621-5334

14. ABSTRACT
Toward creating Hertz–Langmuir–Knudsen (HLK) equations for calculating volatilization rates for energetic materials (EMs) formulated with nitrocellulose (NC), we evaluated a directed-message passing neural network (D-MPNN) model's predictions for the saturated vapor pressures (P_{sat}) of organic nitrate esters. Comparing D-MPNN-predicted and measurement-based values for 32 different alkyl nitrates at temperatures (T) from 250 to 1000 K, we observed reasonable agreement in most cases. Moreover, in cases in which discrepancies were significant, they could be rationalized. Based on those findings, we concluded that the model's $P_{sat}(T)$ predictions warranted use in formulating the HLK equations we sought. Volatilization-rate predictions produced by those equations were compared with values produced by a well-regarded pyrolysis law for double-base propellants. The results indicated that the HLK equations have the potential to produce better predictions for the rate at which (pyrolyzed) NC will volatilize at temperatures less than 400 K. Thus, they may find application in models for simulating the response of NC-containing EMs to thermal loads relevant to ignition and cook-off scenarios.

15. SUBJECT TERMS
Weapons Sciences, deflagration, combustion, vapor pressure, energetic materials

16. SECURITY CLASSIFICATION OF:			17. LIMITATION OF ABSTRACT	18. NUMBER OF PAGES
a. REPORT	b. ABSTRACT	C. THIS PAGE		
UNCLASSIFIED	UNCLASSIFIED	UNCLASSIFIED	UU	40

19a. NAME OF RESPONSIBLE PERSON	19b. PHONE NUMBER *(Include area code)*
Christopher P. Stone	(520) 691-5244

STANDARD FORM 298 (REV. 5/2020)
Prescribed by ANSI Std. Z39.18

Contents

List of Figures iv

List of Tables iv

1. Introduction 1

2. The D-MPNN Model 8

3. Literature Search for Measurement-Based $P_{sat}(T)$ Values 8

3.1 Gray and Pratt (1957) 8

3.2 Kemp et al. (1957) 9

3.3 Fischer and Ballschmiter (1998a, 1998b) 11

3.4 Härtel et al. (2019) 11

4. Comparisons 12

4.1 Gray and Pratt (1957) 12

4.2 Kemp et al. (1957) 14

4.3 Fischer and Ballschmiter (1998a, 1998b) 18

4.4 Härtel et al. (2019) 19

5. $P_{sat}(T)$ Predictions for MNGM, DNGM, and TNGM 20

6. Comparison of Mass Flux Predictions from Pyrolysis Law and HLK Equations 21

7. Summary and Conclusions 23

8. References 24

Appendix. Implementation of the Joback Method for Estimating the Saturated Vapor Pressures of Organic Nitrate Esters 28

List of Symbols, Abbreviations, and Acronyms 33

Distribution List 34

List of Figures

Figure 1. The molecular structures of MNGM, DNGM, and TMGM. 3

Figure 2. Comparison of predicted and measured $P_{sat}(T)$ values for nitroxyethane, 1-nitroxypropane, 2-nitroxypropane, 1-nitroxybutane, and 2-nitroxymethylpropane. 13

Figure 3. Comparison of predicted and measurement-based $P_{sat}(T)$ values for 1,3-dinitroxypropane, 1,3-dinitroxybutane, 1,4-dinitroxybutane, 1,5-dinitroxypentane, 2,4-dinitroxypentane, and 2,5-dinitroxyhexane. 15

Figure 4. Comparison of predicted and measurement-based $P_{sat}(T)$ values for 1,2,4-trinitroxybutane, 1,2,5-trinitroxypentane, and NG. 17

Figure 5. Comparison of predicted and measurement-based $P_{sat}(T)$ values for EGDN, NG, and 1,2,3,4-tetranitroxybutane. 20

Figure 6. The D-MPNN model's $P_{sat}(T)$ predictions for MNGM, DNGM, and TNGM. 21

Figure 7. Comparison of $\dot{m}_{l\rightarrow g}$ predictions: Zenin's (1995) DBP pyrolysis law vs. the HLK equation in the limit $X_{k,g}^{+0} \rightarrow 0$. 22

Figure A-1. Comparison of $P_{sat}(T)$ estimates for NG produced by various methods. 32

List of Tables

Table 1. Antoine equation coefficients for calculating $P_{sat}(T)$ values (in atm) for nitroxyethane, 1-nitroxy-propane, 2-nitroxypropane, 1-nitroxybutane, and 2-nitroxymethylpropane. 9

Table 2. $P_{sat}(T)$ values for alkyl nitrates with two or three nitroxy groups. 10

Table 3. Antoine equation coefficients for calculating $P_{sat}(T)$ values (in atm) for EGDN, NG and 1,2,3,4-tetranitroxybutane 12

Table 4. Comparison of measured and predicted $P_{sat}(T)$ values for alkyl dinitrates. 19

Table A-1. Selected Joback method coefficients for estimating T_{nbp} and $\Delta H_v(T_{nbp})$. 29

Table A-2. Data used to derive $c_{T_{nbp},-ONO_2}$ and $c_{\Delta H_v,-ONO_2}$. 31

1. Introduction

Seeking to accelerate the development of advanced weapon propulsion system concepts, U.S. Army Combat Capabilities Development Command Army Research Laboratory researchers have developed and applied physics-based models with detailed gas-phase finite-rate chemical kinetics mechanisms to simulate the deflagration of nitrocellulose (NC) (Miller and Anderson 2004; Conner et al. 2008; Nusca 2014). Motivated by the creation of a chemical kinetics mechanism (Chen et al. 2021) with the potential to produce more reliable and informative predictions for the decomposition and combustion of NC than prior constructs (Anderson et al. 2011; Chen and McQuaid 2013), the study summarized herein was undertaken with the objective of formulating a physics-based representation for the volatilization process that would supersede the semi-empirical representation utilized to date. In addition, we anticipate that such a representation will facilitate the development of models for predicting NC's response to the thermal loads it will experience in ignition and cook-off scenarios.

Undergirding the development and application of such models, several features of the molecular structure of propellant-grade NC (polymer chains) warrant mentioning. NC is manufactured by nitrating various sources of cellulose, which is a homopolymer of anhydroglucose monomers (GMs) linked by β-1,4 glycosidic linkages (Saunders and Taylor 1990; Hsieh 2007). The GMs have three hydroxyl (-OH) groups: one bonded to the primary C-atom at the 6th position (C6) and one (each) bonded to the secondary C-atoms at C2 and C3. Each hydroxyl group has the potential to be nitroxylated, and propellant-grade NC chains comprise GMs with one, two, and three nitroxy ($-ONO_2$) groups. The relative populations of the three nitrated-GM types depend on the chains' overall level of nitration (Leider and Seaton 1979; Miller and Anderson 2004).

Armed with that knowledge, Miller and Anderson (2004) formulated and combined a set of submodels for simulating the "formidably complex" process by which NC decomposes, volatilizes, and combusts in a deflagration wave. Extrapolated from their seminal work in modeling the deflagration of nitroglycerin (NG) and RDX (Miller and Anderson 2000), the approaches they utilized to simulate volatilization and gas-phase combustion chemistry remain standards for polymer-containing systems and merit review.

Lacking the information necessary to create a well-founded, "detailed" representation for NC's pyrolysis and the earliest stages of the ensuing gas-phase decomposition of its products, Miller and Anderson (2000) utilized a mechanism developed to represent the "small-molecule" reaction chemistry in the "dark zones"

(DZs) of flames of nitrate esters and nitramines burning at low (<10 atm) pressure (Anderson et al. 2011). (No molecule in the DZ mechanism had more than four multi-electron atoms.) Since all the species in the DZ mechanism (except for NO_2 and HONO) were at least two reaction steps removed from molecules likely to be volatilizing from the surface, Miller and Anderson (2000) had to specify (ad hoc) mixtures of species (referred to as nascent product sets [NPSs]) to serve as surrogates. In addition, the disconnect between the actual products of NC's pyrolysis and the species in the DZ mechanism also required that Miller and Anderson utilize a semi-empirical method to calculate the mass flux of the volatilization process. For that, they chose a pyrolysis law,

$$\dot{m}_{l\to g} = A' \exp\left(-\frac{B'}{T}\right), \tag{1}$$

with values for A' (1.8×10^3 g/cm^2) and B' (5000 K) specified based on measured data for double-base propellants (DBPs) that was published by Zenin (1995).

By trial and error, Miller and Anderson (2000) found NPSs for NC that produced pressure-dependent burning rate predictions for standard gun propellants that were in reasonable agreement with measured values. However, as more conclusively demonstrated by comparing the heat release versus distance profiles produced by simulations of NG flames generated by the DZ mechanism and a mechanism that included pathways for the decomposition of the NG (Chen et al. 2019), it was evident that the chemistry occurring close to the burning surface was not well represented by the NPS-DZ mechanism combinations employed, calling into question the value of the model's predictions for a region that is a critically important determinant of burning rates.

Foreseeing benefits that would derive from better representations of the chemical kinetics near the surface of a burning propellant, and believing that NC's pyrolysis in a deflagration wave would proceed through molecules "like" the mono-, di-, and tri-nitrated GM types found in propellant-grade NC, Chen et al. (2021) and McQuaid et al. (2016) expanded the DZ mechanism to include reactions for the decomposition of species designed to represent them. Among the inclusions are reaction networks for decomposing [(3,4,5-trihydroxy)oxan-6-yl]methyl nitrate (MNGM, $C_6H_{11}NO_7$), [(3-nitroxy-4,5-dihydroxy)oxan-6-yl]methyl nitrate (DNGM, $C_6H_{10}N_2O_9$), and [(3,4-dinitroxy-5-hydroxy)oxan-6-yl]methyl nitrate (TNGM, $C_6H_9N_3O_{11}$). Shown in Figure 1, each of these molecules has an -H group in lieu of the glycosidic linkage at C1 and an -OH group in lieu of the glycosidic linkage at C4. Under no illusion that the pyrolysis of NC in a deflagration wave would directly produce MNGM, DNGM, or TNGM; Chen et al. (2021) nonetheless presumed that a mechanism for modeling the decomposition of these three

molecules would offer a better representation for the earliest stages of the process than any construct of which they were aware. This remains to be demonstrated.

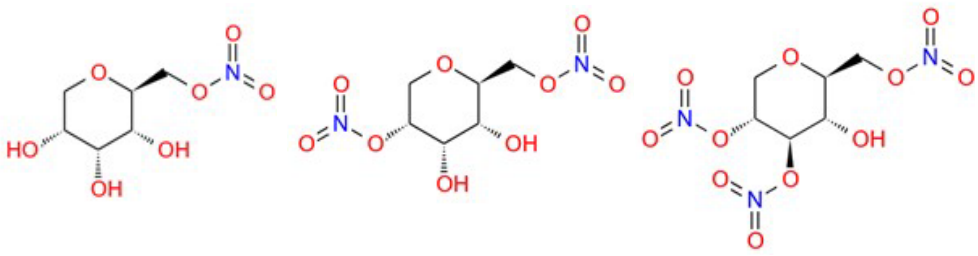

Figure 1. The molecular structures of MNGM, DNGM, and TMGM.

Planning for that effort, Chen et al. (2021) presumed that Zenin's (1995) pyrolysis law would have to be used to calculate the mass flux of volatilization processes involving MNGM, DNGM, and TNGM because, like the NPSs specified by Miller and Anderson (2004), they were (still) merely representative of the molecules near the interface between the condensed and gas phases in a deflagration wave. Likewise, needing to address that same issue in formulating a model for simulating NC's response to the conditions imposed during a heat-wait-seek experiment performed with an accelerating rate calorimeter (Turcotte et al. 2006), and lacking an obvious alternative, McQuaid et al. (2016) used it for that purpose. However, the model's prediction for the pressurization rate was poor. In the experiment, no evidence of gasification was observed until the sample reached approximately 400 K, when thermal runaway and rapid pressurization occurred. The model, on the other hand, predicted the starting NC sample would completely gasify by 350 K.

In that particular case, the discrepancy between predicted and measured system pressures was clearly attributable to the model's use of Equation 1 for calculating $\dot{m}_{l\to g}$. Prescribing an irreversible process, it produced a positive volatilizing flux irrespective of the system's relationship to phase equilibrium, where the net volatilization rate is zero. Since the concentration of gas-phase NC polymer chains in a two-phase system is effectively zero at temperatures below which NC decomposes, NC is essentially in phase equilibrium at such temperatures. Moreover, based on standard calorimetry experiments (Jones et al. 2003; Turcotte et al. 2006; Sućeska et al. 2010), NC does not begin to decompose at appreciable rates until temperatures exceed approximately 400 K. Therefore, it was not particularly surprising that the use of Equation 1 at temperatures below this limit would yield poor predictions.

Recognizing the limitations of pyrolysis laws (in general), McQuaid and coworkers began to formulate and apply Hertz–Langmuir–Knudsen (HLK) equations to calculate $\dot{m}_{l\to g}$ in systems for which they appeared to be a credible representation

of the process and their formulation was feasible (McQuaid and Chen 2016a, 2016b; McQuaid et al. 2017). Following Miller (1997), HLK equations have the form

$$\dot{m}_{l\to g} = \sum_k \propto_k (W_k/2\pi RT^0)^{\frac{1}{2}}\left(X_{k,g}^{-0}P_{sat}^0 - X_{k,g}^{+0}P\right), \quad (2)$$

where $\propto_k$ is the "sticking coefficient" of species k, W_k is its molecular weight (MW), R is the universal gas constant, T^0 is the temperature of the interface, $X_{k,g}^{-0}$ is k's mole fraction on the condensed-phase side of the interface, P_{sat}^0 is the material's saturated vapor pressure at T^0, $X_{k,g}^{+0}$ is k's mole fraction on the gas-phase side of the interface, and P is the gas-phase's pressure. In the absence of gas-phase reaction chemistry, the term $\left(X_{k,g}^{-0}P_{sat}^0 - X_{k,g}^{+0}P\right)$ (and therefore $\dot{m}_{l\to g}$) will go to zero. As such, Equation 2 has the potential to be more representative of volatilization rates as temperatures approach those at which reaction rates become negligible. However, the formulation of such representations requires that one be able to produce reasonable estimates for $X_{k,g}^{-0}$ and $P_{sat}(T)$, and that is only straightforward for systems in which 1) it is reasonable to assume that the parent molecules in the condensed phase volatilize directly (i.e., without first decomposing) and 2) $P_{sat}(T)$ values for the parent molecules have been measured or may be reliably and affordably estimated.

Energetic materials (EMs) for which HLK equations have been successfully developed and applied in a CYCLOPS model include methyl nitrate (McQuaid and Chen 2016a, 2016b), NG (Chen et al. 2018), RDX (Veals et al. 2019), and HMX (Chen et al. 2021). In each of these cases, the direct volatilization of the parent molecule from the condensed phase was expected, measured $P_{sat}(T)$ values could be found, and the burning rate predictions produced by the CYCLOPS model were compelling. Moreover, when integrated into models of processes occurring at temperatures much lower than those observed at the surface of a deflagrating EM, the HLK equations that were developed for RDX and NG yielded compelling predictions for those processes as well (McQuaid et al. 2017, 2021).

Compared with those cases, the formulation of an HLK equation for a polymer-containing formulation is much more difficult. The $P_{sat}(T)$ values tend to be inversely proportional to a molecule's MW, and, compared with the MWs of molecules for which HLK equations have been successfully developed (i.e., MW <300 amu), those of (intact) polymer chains are huge. In the case of EM-grade NC, chain MWs range from 20,000 to 30,000 amu (Saunders and Taylor 1990). Therefore, even at the temperatures typical of the surface of a deflagrating EM, $P_{sat}(T)$ values for polymers are negligibly small relative to values needed for HLK-based $\dot{m}_{l\to g}$ estimates to approach those observed in experiments. Rather, as found experimentally, the chains must first decompose to smaller molecules, and

currently there are no practical methods for reliably predicting the chemical evolution of polymer pyrolysis. In addition, the estimation of $P_{sat}(T)$ values for multicomponent mixtures is likewise problematic, further adding to the difficulty.

The idea that we might profitably develop an HLK equation for a mixture of MNGM, DNGM, and TNGM was sparked by a recent study that was conducted to evaluate various models of the deflagration of hydroxyl-terminated polybutadiene (HTPB) (type R45M) in an opposed-flow burner (Stone et al. 2024). Like NC, HTPB comprises polymer chains that must decompose to smaller molecules to volatilize at rates observed experimentally, and there were no practical methods for modeling HTPB's pyrolysis that could serve as a basis for specifying $\{X_{k,g}^{-0}\}$. Intuiting nonetheless that HTPB's pyrolysis would proceed through relatively large hydrocarbon fragments with molecular structures similar to HTPB, Chen and McQuaid (2009) developed and applied a mechanism predicated on the end-state of HTPB's pyrolysis in a deflagration wave being reasonably well represented by 6-ethenyl-2,8,12,16-octadectetraene (EODT, $C_{20}H_{32}$).

Like MNGM, DNGM, and TNGM, EODT was a notional molecule that was merely expected to be representative of the intermediates through which HTPB would decompose before volatilizing. Therefore, it was assumed when the mechanism to represent its decomposition and combustion was developed that an empirical prescription would have to be specified to calculate its $\dot{m}_{l\rightarrow g}$. Employed to simulate the deflagration and combustion of a wide range of HTPB-containing formulations (McQuaid et al. 2023 and references therein), such prescriptions proved to work well. Nonetheless, C.P.S. wondered whether reasonable predictions would be produced by a model that had an HLK equation predicated on HTPB's pyrolysis by the deflagration wave producing pure liquid EODT at the surface.

As already mentioned, the formulation of an HLK representation requires that one be able to reasonably estimate a compound's $P_{sat}(T)$ values, and with EODT being a notional molecule, there was no possibility that its $P_{sat}(T)$ values could be affordably measured. To address that issue, we utilized the Joback (group additivity) method to obtain estimates for its normal boiling point [T_{nbp}, where $P_{sat}\left(T_{nbp}\right) = 1$ atm] and enthalpy of vaporization at T_{nbp} [$\Delta H_v\left(T_{nbp}\right)$] (Joback and Reid 1987). Those estimates were then substituted into an integrated form of the Clausius-Clapeyron equation,

$$\ln[P_{sat}(T)] \approx \frac{T*\Delta H_v\left(T_{nbp}\right)-T_{nbp}*\Delta H_v(T)}{R*T_{nbp}*T} \approx \frac{\Delta H_v\left(T_{nbp}\right)*(T-T_{nbp})}{R*T_{nbp}*T}, \qquad (3)$$

to estimate $P_{sat}(T)$. Integrated with a CYCLOPS model, the HLK equation derived from those estimates produced predictions that proved to be in better agreement with measured values for various parameters of the gas-phase flame—including

temperature and CO's mole fraction as a function of distance from the surface—than those produced with semi-empirical prescriptions (Stone et al. 2024).

In view of that outcome, we believed that the development of HLK equations for calculating the volatilization rates of MNGM, DNGM, and TNGM was worth undertaking. However, because they were notional molecules, there was no possibility that their $P_{sat}(T)$ values could be affordably measured. Therefore, computational methods for generating estimates had to be identified and evaluated.

Being low cost and straightforward to implement, the Joback method was evaluated first, with estimates it produced for NG's T_{nbp} and $\Delta H_v(T_{nbp})$ serving as tests of its validity for nitrate esters (Joback and Reid 1987). (See the Appendix for the implementation of the Joback method for nitrate esters.) Because NG rapidly decomposes at temperatures below which it will boil at 1 atm, the estimates were not verifiable.* Nonetheless, the extrapolation to higher temperatures of $P_{sat}(T)$ values measured at temperatures less than 330 K suggested that NG's T_{nbp} would be approximately 500 K (see Section 4). The Joback-based estimate was 790 K (Joback and Reid 1987). In addition, the Joback-based $\Delta H_v(T_{nbp})$ estimate (27 kcal/mol) was somewhat higher than $\Delta H_v(T)$ values derived from $P_{sat}(T)$ values measured at lower temperatures (25 kcal/mol) (Joback and Reid 1987). Since $\Delta H_v(T)$ values tend to decrease with an increase in temperature, going to 0 kcal/mol at the critical point, the method's capacity to estimate this parameter for nitrate esters was also suspect. Therefore, we were skeptical that T_{nbp} and $\Delta H_v(T_{nbp})$ estimates produced by the method would yield reasonable $P_{sat}(T)$ estimates for MNGM, DNGM, and TNGM. (Additions to the Joback method [Joback and Reid 1987] that appear to improve its T_{nbp} and $\Delta H_v(T_{nbp})$ predictions for nitrate esters are presented in the Appendix.)

Considering alternatives, we believed that, as was found for EODT (Veals et al. 2023), $\Delta H_v(T)$ estimates for MNGM, DNGM, and TNGM could be derived from results produced by atomistic molecular dynamics simulations. However, their generation and analysis would have been costly (labor wise) and taken 6 months to complete. Moreover, we would still be faced with estimating each of their $P_{sat}(T)$

* We believe that (in principle) NG has a "normal boiling point" as that concept is defined: that is, a two-phase system of pure NG in which $P_{sat}(T_{nbp})$ is 1 atm. However, its measurement would require a technique that could produce a two-phase system in equilibrium at T_{nbp} within a temporal interval that was short relative to the time scale for NG's decomposition at that temperature. (In a homogeneous reactor simulation performed to estimate the latter, 1 wt% NG of a 1-atm gas-phase sample at 500 K decomposed within approximately 10 ms.) We are unaware of any such technique having ever been developed and applied. Nevertheless, the compelling burning rate predictions for NG produced by a CYCLOPS model with an HLK equation suggest that phase equilibrium between the liquid and gas is being approached near their interface in NG's deflagration (Chen et al. 2018). See McQuaid et al. (2015) for additional discussion of this matter.

values at some (one) temperature, and we were unaware of any simple reliable methods available for that purpose. Therefore, such an undertaking could not be justified.

Offering an alternative to these standard methods for $P_{sat}(T)$ estimation, a directed-message passing neural network (D-MPNN) that Lansford et al. (2023) trained with a physics-informed transfer learning strategy was considered next. Interested in establishing the strategy's potential to produce reasonable property predictions for EMs outside the domain of the generic hydrocarbon sets that were readily available for training it, they used the strategy to develop a model for predicting $P_{sat}(T)$ values. Validating the model on an out-of-sample test set that included EMs with $P_{sat}(T)$ values that were much lower than those in the training set, they found that it produced predictions whose accuracies were comparable to those of experiments.

Despite that conclusion, M.J.M. was concerned about the D-MPNN model's capacity to predict $P_{sat}(T)$ values for MNGM, DNGM, and TNGM because only two nitrate esters were in the validation set (i.e., NG and 1,2-dinitroxyethane [EGDN]), and the model's $P_{sat}(298)$ prediction for NG was more than 1 order of magnitude larger than a nominal value derived from measured data. In addition, temperatures at the surface of NC burning in a rocket motor can be expected to range from 500 to 1000 K, and there was no validation of the D-MPNN model's $P_{sat}(T)$ predictions for any specific molecule at a temperature other than 298 K. Therefore, additional validation of the model's predictions for nitrate esters was considered necessary.

Toward that objective, we conducted a literature search and found measurement-based $P_{sat}(T)$ values for 32 different alkyl nitrates. $P_{sat}(T)$ predictions for all of them were generated at temperatures from 250 to 1000 K. In majority of cases, the agreement between D-MPNN-predicted and measurement-based values was reasonable. Moreover, in cases where discrepancies were significant, they could be rationalized.

Based on those findings, we concluded the model's predictions for MNGM, DNGM, and TNGM warranted use in formulating the desired HLK equations. Predictions produced by those equations were compared to the predictions produced by Zenin's (1995) pyrolysis law. The results indicated that the HLK equations have the potential to produce better predictions for the rate of NC's volatilization at temperatures less than 400 K. Therefore, they may find application in models for simulating the ignition and response to cook-off of EMs formulated with NC.

2. The D-MPNN Model

A detailed description of the D-MPNN model is provided elsewhere (Lansford et al. 2023). Briefly, using as inputs only 1) the graph structure of a molecule, 2) generic atom and bond-level features, and 3) temperature, Lansford et al. (2023) explored several architectures for "augmenting" a $P_{sat}(T)$ data training set that would facilitate the data's extrapolation outside the domain within which they were measured. Lansford et al. (2023) found that a model produced by a two-temperature representation training regimen, where one temperature is passed into a physical equation embedded in the D-MPNN, outperformed all others. Results produced by that model are presented.

3. Literature Search for Measurement-Based $P_{sat}(T)$ Values

Utilizing Google and the Web-of-Science search engines, we sought peer-reviewed publications of measurement-based $P_{sat}(T)$ values for organic nitrate esters to which the D-MPNN model's predictions could be compared. However, $P_{sat}(T)$ values for nitrate esters with three or more carbon atoms and two or more nitroxy groups are relatively low at 298 K, which makes them difficult to measure accurately. (See Ostmark et al. [2012] for a review of the measurement of $P_{sat}(T)$ values for EMs.) In addition, the time scale for the decomposition of nitrate esters at temperatures that would yield readily measurable $P_{sat}(T)$ values generally precludes that possibility. As a result, we did not expect to find a large amount of validating data, and that proved to be the case. Data published by Gray and Pratt (1957), Kemp et al. (1957), Fischer and Ballschmiter (1998a), and Härtel et al. (2019) appeared to be the best available. The subsections that follow discuss our assessment of their reliability and applicability for validating the D-MPNN model's $P_{sat}(T)$ predictions for MNGM, DNGM, and TNGM. The representations of the published data that were the basis for plotting them are also provided.

3.1 Gray and Pratt (1957)

Gray and Pratt (1957) published $P_{sat}(T)$ values for six small (mono)nitroxy-functionalized molecules at 10-K intervals from 273 to 343 K. The molecules were nitroxymethane, nitroxyethane, 1-nitroxypropane, 2-nitroxypropane, 1-nitroxybutane, and 2-nitroxymethyl-propane. Except for the data for nitroxymethane, Gray and Pratt (1957) fit to them the Antoine equation:

$$\log_{10}\left(\frac{P_{sat}}{1\ \text{atm}}\right) = A - \frac{B}{(T+C)}\,, \tag{4}$$

where A, B, and C are constants and T is temperature in K.† For convenience, the coefficients derived from those fits are provided in Table 1. They are the basis for the plots of the data that are presented in Section 4. Those plots include $P_{sat}(T)$ values generated for temperatures ranging from 250 to 1000 K to see how the D-MPNN model's predictions would compare to them over the entire temperature range pertinent to predicting a propellant's performance and vulnerability.

Table 1. Antoine equation coefficients for calculating $P_{sat}(T)$ values (in atm) for nitroxyethane, 1-nitroxy-propane, 2-nitroxypropane, 1-nitroxybutane, and 2-nitroxymethylpropane.[a]

Compound	SMILES	*A*	*B* (K)	*C* (K)	Temp (K)
nitroxyethane	CCO[N+](=O)[O-]	4.27952	1337.035	−48.37	273–343
1-nitroxypropane	CCCO[N+](=O)[O-]	4.85638	1721.723	−27.66	273–343
2-nitroxypropane	CC(O[N+](=O)[O-])C	3.53925	1018.568	−89.622	273–343
1-nitroxybutane	CCCCO[N+](=O)[O-]	5.46362	2177.065	−4.855	273–343
2-nitroxymethylpropane	CC(C)CO[N+](=O)[O-]	5.31960	2045.425	−8.996	273–343

[a] Derived from $P_{sat}(T)$ values published by Gray and Pratt (1957). Temp = temperature.

Assessing the data's reliability, we noted that Gray and Pratt (1957) provided a detailed summary of the procedures they utilized to prepare and analyze each sample. In addition, they measured the $P_{sat}(T)$ values directly with a mercury manometer, which, given the $P_{sat}(T)$ values of the subject compounds in the temperature range studied, was appropriate. Thus, we had a high degree of confidence in the data's reliability. However, because the molecules were small relative to MNGM, DNGM, and TNGM, and they had only one nitroxy group, their relevance with respect to validating the D-MPNN model's $P_{sat}(T)$ predictions for MNGM, DNGM, and TNGM was considered limited.

3.2 Kemp et al. (1957)

Kemp et al. (1957) published $P_{sat}(293)$, $P_{sat}(303)$, and $P_{sat}(313)$ values for nine alkyl nitrates that had either two or three nitroxy groups. The compounds were 1,3-dinitroxypropane, 1,3-dinitroxybutane, 1,4-dinitroxybutane, 1,5-dinitroxypentane, 2,4-dinitroxypentane, 2,5-dinitroxyhexane, 1,2,4-trinitroxybutane, 1,2,5-trinitroxypentane, and NG. (For NG, Kemp et al. [1957] utilized two different methods to synthesize samples and reported $P_{sat}(T)$ values for each product, labeling them I and II.)

† Gray and Pratt (1957) fit an alternate expression to their $P_{sat}(T)$ data for nitroxymethane. Believing that—with respect to validating the D-MPNN model's $P_{sat}(T)$ predictions for MNGM, DNGM, and TNGM—the relevance of these data would be very limited, we decided not to include them as a basis for the evaluation.

For the comparisons, we plotted the average of the individual $P_{sat}(T)$ values reported for each compound at each temperature. The average values are provided in Table 2. In addition, we fit Equation 4 (with $C = 0$) to the data for each molecule and plotted the $P_{sat}(T)$ values it generated for temperatures ranging from 250 to 1000 K. (The coefficients are provided in the Appendix.)

Table 2. $P_{sat}(T)$ values for alkyl nitrates with two or three nitroxy groups.[a]

Compound	SMILES	$P_{sat}(T)$ (atm × 10^6)		
		293 K	303 K	313 K
1,3-dinitroxypropane	O=[N+]([O-])OCCCO[N+](=O)[O-]	21.7	54.6	152.6
1,3-dinitroxybutane	CC(CCO[N+](=O)[O-])O[N+](=O)[O-]	28.9	67.1	188.6
1,4-dinitroxybutane	O=[N+]([O-])OCCCCO[N+](=O)[O-]	12.0	26.3	53.9
1,5-dinitroxypentane	O=[N+]([O-])OCCCCCO[N+](=O)[O-]	6.1	18.0	48.0
2,4-dinitroxypentane	CC(CC(C)O[N+](=O)[O-])O[N+](=O)[O-]	38.2	94.7	184.2
2,5-dinitroxyhexane	CC(CCC(C)O[N+](=O)[O-])O[N+](=O)[O-]	1.6	10.0	35.8
1,2,4-trinitroxybutane	O=[N+]([O-])OCCC(CO[N+](=O)[O-])O[N+](=O)[O-]	1.4	3.3	7.0
1,2,5-trinitroxypentane	O=[N+]([O-])OCCCC(CO[N+](=O)[O-])O[N+](=O)[O-]	0.21	0.38	0.63
NG I	O=[N+]([O-])OCC(CO[N+](=O)[O-])O[N+](=O)[O-]	0.27	1.1	4.3
NG II		0.26	1.4	4.7

[a] Average of values published by Kemp et al. (1957).

Assessing these data's reliability, we noted that Kemp et al. (1957) provided a summary of the procedures they used to prepare each sample, establish its chemical composition, and derive $P_{sat}(T)$ values from the values of the parameters measured in the experiments. Therefore, we had a fair degree of confidence in their reliability. However, sample preparation and characterization appeared to be more difficult than it was for the mononitrated compounds whose properties were characterized by Gray and Pratt (1957). Moreover, the $P_{sat}(T)$ values of the compounds studied by Kemp et al. (1957) were several orders of magnitude lower than those that were measured by Gray and Pratt (1957), preventing them from being measured directly. Instead, they were derived from a transpiration method that involved measuring the reduction in a sample's mass produced by flowing a carrier gas over it. As such, Kemp et al. (1957) had to make some assumptions about the relationship between this dynamic system and the equilibrium system of interest, and we considered them to be potential sources of systematic error.

Among the assumptions Kemp et al. (1957) made in deriving $P_{sat}(T)$ values from the parameter values they measured were the applicability of the ideal gas law and Dalton's law of partial pressure. Given the size of the molecules they studied and the potential for gas-phase nitroxy-functionalized molecules to interact with one another, we viewed these assumptions with some skepticism and had less confidence in the accuracies of these data than those of Gray and Pratt (1957).

Of particular concern was the $P_{sat}(T)$ values Kemp et al. (1957) reported for 1,2,5-trinitroxypentane. Compared to all other $P_{sat}(T)$ values they published, the values

for 1,2,5-trinitroxypentane were among the lowest, and the $\Delta H_v(303)$ value derived from them (10.0 ± 0.5 kcal/mol) was the lowest of the set. We expected the latter to be among the highest; similar to, if not greater than, the average of the two values Kemp et al. (1957) found for NG (25.5 kcal/mol). Taken together, these observations suggested to us that the relative uncertainty in $P_{sat}(T)$ values less than approximately 5×10^{-7} atm was higher than Kemp et al. (1957) supposed. That conclusion notwithstanding, the sizes of the molecules in this set approached those of MNGM, DNGM, and TNGM and they had two or three nitroxy groups. Therefore, with respect to validating the D-MPNN model's $P_{sat}(T)$ predictions for MNGM, DNGM, and TNGM, we considered these data more relevant than Gray and Pratt's (1957).

3.3 Fischer and Ballschmiter (1998a, 1998b)

Fischer and Ballschmiter (1998a, 1998b) published $P_{sat}(298)$ values for 23 alkyl dinitrates.[‡] The values were derived from experiments performed with a gas chromatograph in which a "retention index" (*RI*) for each compound was calculated, then making the assumption that each compound's $P_{sat}(298)$ value was proportional to its *RI*. As such it was essentially a transpiration method, and the derivation of $P_{sat}(T)$ values from *RI*s presumably required comparing them to some standard. However, Fischer and Ballschmiter (1998a, 1998b) do not discuss this aspect of their method, making it difficult for us to assess the degree of uncertainty in the absolute values of their results. Nonetheless, the trends in the $P_{sat}(298)$ values as a function of molecular size and structure were consistent with our expectations. Thus, they were considered suitable for the purpose of validating the D-MPNN model's predictions for MNGM, DNGM, and TNGM.

3.4 Härtel et al. (2019)

Härtel et al. (2019) published $P_{sat}(T)$ values for EGDN, NG, and 1,2,3,4-tetranitroxybutane that they derived from a transpiration method. They also summarized previously published $P_{sat}(T)$ values for EGDN and NG. The

[‡] The referenced Fischer and Ballschmiter (1998a, 1998b) papers present the exact same $P_{sat}(298)$ data. There were 23 distinct molecules in the set, but three were listed twice and distinguished by the labels "*c*-" or "*t*-" in the 1998a paper. In the 1998b paper, one of those three pairs was identified as comprising "diastereomers." We assumed the labels stood for "cis-" and "trans-," respectively. However, one molecule was a linear alkane (without a double bond), and the other two were nonaromatic rings without any double bonds. Thus, we were not sure what distinguished the "*c*-" structure from the "*t*" structure, and we were unable to find the answer in Fischer and Ballschmiter's (1998a, 1998b) papers. Observing that the differences in the $P_{sat}(T)$ values for a given *c*-*t* pair were relatively small, we decided not to investigate the matter further and simply specified one SMILES string for each pair.

$P_{sat}(298)$ values they found for these two compounds were approximately 20% higher than the respective average of the previously published values. Thus, we had a fair degree of confidence in their reliability. For the purposes of this study, we fit Equation 4 with $C = 0$ to the $P_{sat}(T)$ values derived from individual experiments that Härtel et al. (2019) provided as supporting information. The coefficients we obtained for each compound on that basis are shown in Table 3.

Table 3. Antoine equation coefficients (with $C = 0$) for calculating $P_{sat}(T)$ values (in atm) for EGDN, NG and 1,2,3,4-tetranitroxybutane

Compound	SMILES	*A*	*B* (K)	*T* (K)
EGDN	O=[N+]([O-])OCCO[N+](=O)[O-]	7.518	3411.9	274–318
NG	O=[N+]([O-])OCC(CO[N+](=O)[O-])O[N+](=O)[O-]	9.004	4501.9	283–328
1,2,3,4-tetranitroxybutane	O=[N+]([O-])OCC(O[N+](=O)[O-])C(CO[N+](=O)[O-])O[N+](=O)[O-]	9.057	4966.8	338–368

Note: Derived from $P_{sat}(T)$ values published by Härtel et al. (2019).

4. Comparisons

4.1 Gray and Pratt (1957)

Figure 2 compares the D-MPNN model's $P_{sat}(T)$ predictions for nitroxyethane, 1-nitroxypropane, 2-nitroxypropane, 1-nitroxybutane, and 2-nitroxymethylpropane to Antoine equation representations of the $P_{sat}(T)$ values that Gray and Pratt (1957) measured. Figure 2 also shows $P_{sat}(T)$ estimates calculated by the Antoine equation at temperatures outside of the ranges within which Gray and Pratt (1957) measured values. In all cases, the D-MPNN's predictions were slightly lower than the measured values in the temperature range within which the measurements were made. However, overall, we were satisfied with the agreement and concluded that further validation of the D-MPNN's predictions for organic nitrate esters with more than one nitroxy group was warranted.

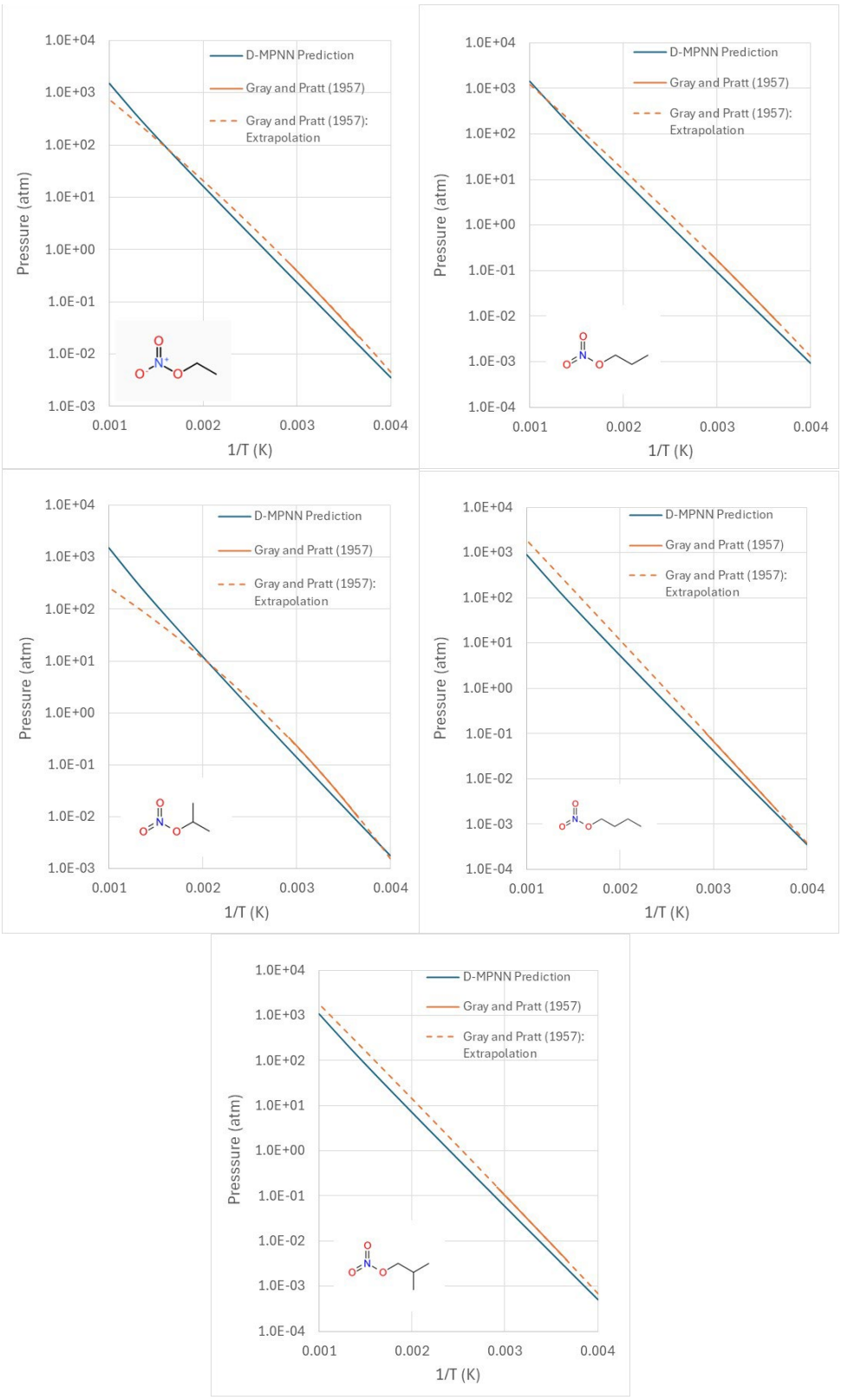

Figure 2. Comparison of predicted and measured $P_{sat}(T)$ values for nitroxyethane, 1-nitroxypropane, 2-nitroxypropane, 1-nitroxybutane, and 2-nitroxymethylpropane.

4.2 Kemp et al. (1957)

Figure 3 compares the D-MPNN model's $P_{sat}(T)$ predictions for six alkyl dinitrates to averages of data published by Kemp et al. (1957). In all of these cases, the predictions were slightly higher than the measurement-based values in the temperature range within which the measurements were made (293–313 K). In addition, the (slight) curvatures in the plots of the predictions were the opposite of what was expected. The slopes of such plots are proportional to the enthalpy of vaporization [ΔH_v], and ΔH_v values tend to decrease with an increase in temperature. Therefore, we expected the slopes' magnitudes would tend toward zero with a decrease in T^{-1} as exhibited in the Antoine equation representations of Gray and Pratt's (1957) data (Figure 2). Nonetheless, except for 2,5-dinitroxyhexane, we considered the agreement between predicted and measurement-based values to be reasonable at temperatures expected near the surface of a burning DBP (500–1000 K).

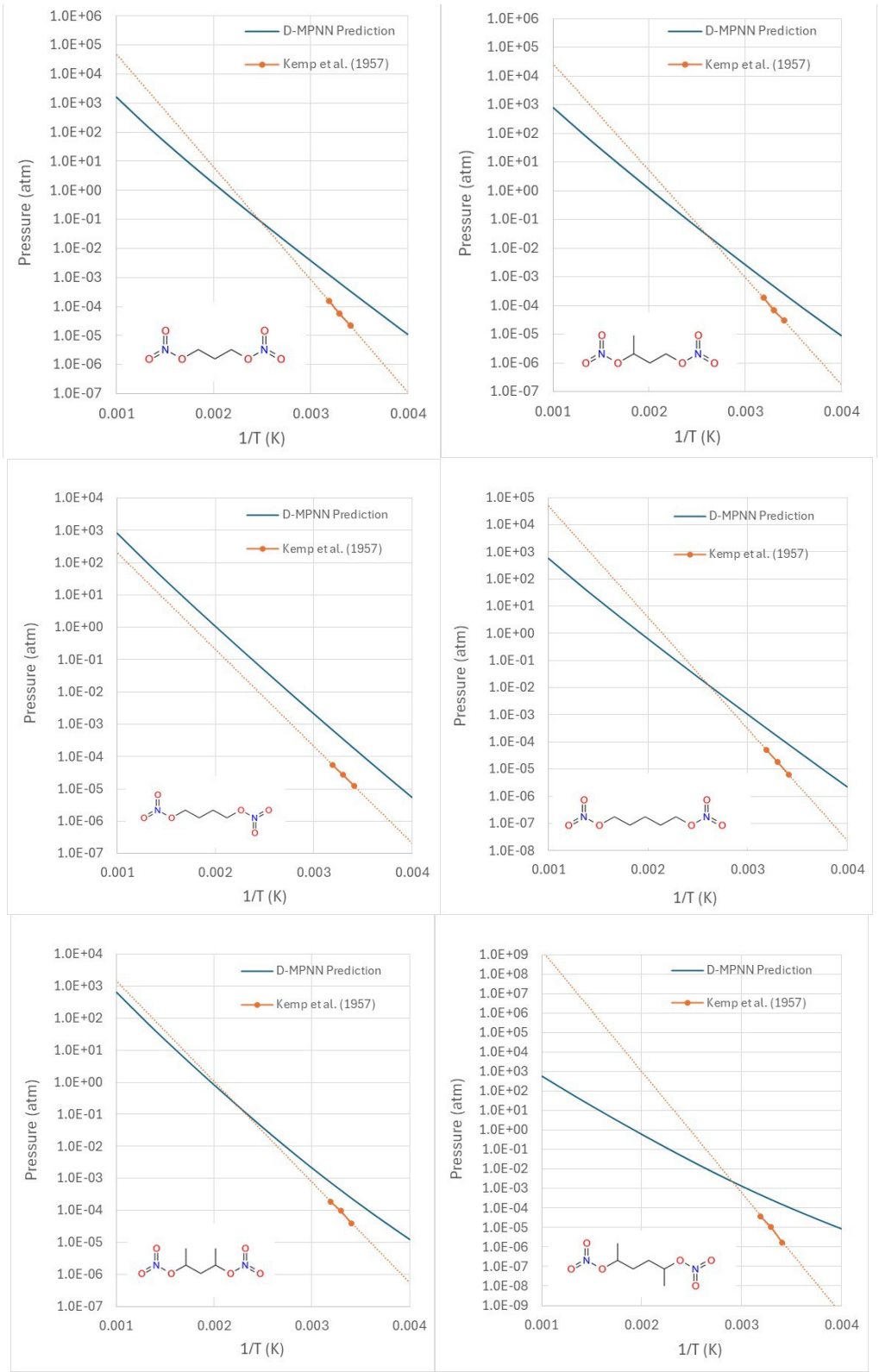

Figure 3. Comparison of predicted and measurement-based $P_{sat}(T)$ values for 1,3-dinitroxypropane, 1,3-dinitroxybutane, 1,4-dinitroxybutane, 1,5-dinitroxypentane, 2,4-dinitroxypentane, and 2,5-dinitroxyhexane.

Regarding the results for 2,5-dinitroxyhexane, we noted that Kemp et al. (1957) derived an enthalpy of *sublimation* [$\Delta H_{sub}(303)$ = 26.2 kcal/mol] from their measurement-based $P_{sat}(T)$ values, and they derived an $\Delta H_v(303)$ value (13.0 kcal/mol) by subtracting from $\Delta H_{sub}(303)$ their finding for the compound's enthalpy of fusion. The $\Delta H_v(300)$ value derived from the $P_{sat}(T)$ value predicted by the D-MPNN model (12.3 kcal/mol) was in reasonable agreement with that result.

That agreement notwithstanding, of all the compounds whose properties were measured by Kemp et al. (1957), 2,5-dinitroxyhexane was the only one for which they derived a $\Delta H_v(303)$ value in that manner, and they do not explain their rationale for doing so. Thus, we were left to assume that 2,5-dinitroxyhexane is a solid at temperatures up to 313 K. Similarly, as is discussed in Section 4.3, Fischer and Ballschmiter (1998a, 1998b) assumed that alkyl dinitrates with six or more carbon atoms are solids at 298 K. This presumption is of course relevant to MNGM ($C_6H_{11}NO_7$), DNGM ($C_6H_{10}N_2O_9$), and TNGM ($C_6H_9N_3O_{11}$).

Figure 4 presents the D-MPNN model's $P_{sat}(T)$ predictions for the three alkyl trinitrates whose $P_{sat}(T)$ values were published by Kemp et al. (1957). The agreements between predicted and measurement-based values for 1,2,4-trinitroxybutane and NG were encouraging. In the case of NG, as mentioned in the introduction, the D-MPNN model's $P_{sat}(298)$ prediction was more than 1 order of magnitude higher than the measurement-based value to which Lansford et al. (2023) compared it, and that was considered cause for concern. As shown in Figure 4, the discrepancy between the D-MPNN model's $P_{sat}(T)$ predictions and the values published by Kemp et al. (1957) near 298 K was similar. However, the agreement improved at slightly higher temperatures, and over the entire temperature range considered (250–1000 K), we thought the predictions would constitute an adequate basis upon which to derive a formula for calculating $P_{sat}(T)$ in an HLK equation.

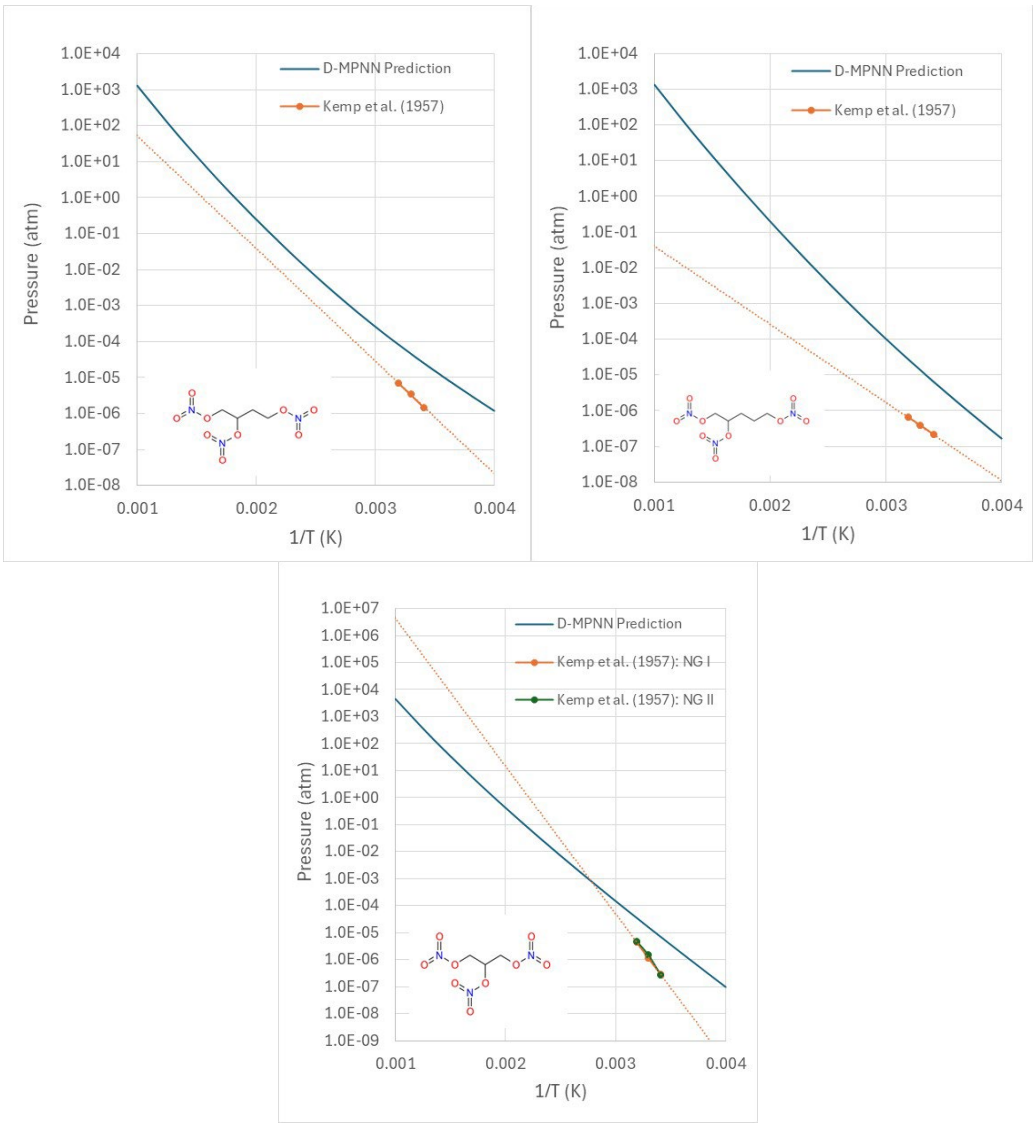

Figure 4. Comparison of predicted and measurement-based $P_{sat}(T)$ values for 1,2,4-trinitroxybutane, 1,2,5-trinitroxypentane, and NG.

Regarding the discrepancy between predicted and measurement-based $P_{sat}(T)$ values for 1,2,5-trinitroxypentane, as noted in Section 3.2, the $\Delta H_v(303)$ value Kemp et al. (1957) derived for it from the $P_{sat}(T)$ values was much lower than expected. Observing also that the $P_{sat}(T)$ values Kemp et al. (1957) found for 1,2,5-trinitroxypentane were the lowest of all of those that they published, we believed the discrepancy may have been due to those values being near the limit of detection of their measurement technique. Thus, the lack of agreement between the measured and predicted values for this compound was not considered cause for concern.

As a final note, in the course of plotting the comparisons shown in Figure 4, we observed (for the first time) that the $P_{sat}(1000)$ predictions for all of them were

within a factor of 2 of 1000 atm, and that proved to be the case for the vast majority of the compounds considered in this study. Given the wide range of sizes of the molecules for which $P_{sat}(1000)$ predictions were produced, and the many orders of magnitude difference in the predictions for them at temperatures near 300 K, this finding was surprising. To the extent the model predicts $P_{sat}(1000)$ is approximately 1000 atm, it suggests the relationship

$$B \approx (A - 3) * (1000 + C) \quad (5)$$

exists among A, B, and C in Equation 4. The proportionality between B (which correlates with ΔH_v) and A (which correlates with P_{sat} at "high" temperatures) is evident in the Antoine equations representing the measured data (see Table A-2 in the Appendix).

4.3 Fischer and Ballschmiter (1998a, 1998b)

Table 4 compares D-MPNN-predicted and Fischer and Ballschmiter's (1998a, 1998b) measurement-based $P_{sat}(298)$ values for 23 alkyl dinitrates. Unlike its predictions relative to those published by Kemp et al. (1957), the D-MPNN model's $P_{sat}(298)$ predictions for molecules with up to five carbon atoms were lower than the respective value Fischer and Ballschmiter (1998a, 1998b) published. However, agreements tended to improve as the number of carbon atoms increased. We were also encouraged by the fact that, with the exception of the $P_{sat}(298)$ prediction for EGDN, the trends in the measured and predicted $P_{sat}(298)$ and $\Delta H_v(298)$ values as a function of the number of carbon atoms and the positions of the nitroxy groups were the same. For example, we observed that for the four dinitroxybutane (DNB) isomers in the table, both measurement-based and model-predicted P_{sat} values had relative magnitudes in the order: $P_{sat}(2{,}3 - DNB) > P_{sat}(1{,}2 - DNB) > P_{sat}(1{,}3 - DNB) > P_{sat}(1{,}4 - DNB)$. Appreciating also that the compounds in this set were similar in size to MNGM, DNGM, and TNGM, we took the comparisons to be further evidence supporting the use of the D-MPNN model for predicting MNGM's, DNGM's, and TNGM's $P_{sat}(T)$ values.

Table 4. Comparison of measured and predicted $P_{sat}(T)$ values for alkyl dinitrates.

Compound	SMILES	$P_{sat}(298)$ atm × 10^5		$\Delta H_v(298)$ kcal/mol
		F&B[a]	D-MPNN	D-MPNN
EGDN[b]	O=[N+]([O-])OCCO[N+](=O)[O-]	152	9.6	12.6
1,3-dinitroxypropane[c]	O=[N+]([O-])OCCCO[N+](=O)[O-]	69	15.6	12.1
1,4-dinitroxybutane[c]	O=[N+]([O-])OCCCCO[N+](=O)[O-]	21	5.2	12.2
1,5-dinitroxypentane[c]	O=[N+]([O-])OCCCCCO[N+](=O)[O-]	6.4	1.7	12.6
1,6-dinitroxyhexane	O=[N+]([O-])OCCCCCCO[N+](=O)[O-]	1.7	1.3	13.1
1,7-dinitroxyheptane	O=[N+]([O-])OCCCCCCCO[N+](=O)[O-]	0.4	0.38	13.8
1,8-dinitroxyoctane	O=[N+]([O-])OCCCCCCCCO[N+](=O)[O-]	0.073	0.15	14.5
1,10-dinitroxydecane	O=[N+]([O-])OCCCCCCCCCCO[N+](=O)[O-]	0.001	0.04	16.1
1,2-dinitroxypropane	CC(CO[N+](=O)[O-])O[N+](=O)[O-]	148.5	28.3	11.7
1,2-dinitroxybutane	CCC(CO[N+](=O)[O-])O[N+](=O)[O-]	62	11.2	11.7
1,2-dinitroxypentane	CCCC(CO[N+](=O)[O-])O[N+](=O)[O-]	23.5	5.4	12.2
1,2-dinitroxyhexane	CCCCC(CO[N+](=O)[O-])O[N+](=O)[O-]	8.1	2.8	12.7
1,2-dinitroxyoctane	CCCCCCC(CO[N+](=O)[O-])O[N+](=O)[O-]	0.90	0.93	13.7
1,2-dinitroxydecane	CCCCCCCCC(CO[N+](=O)[O-]) O[N+](=O)[O-]	0.11	0.15	14.9
1,3-dinitroxybutane[c]	CC(CCO[N+](=O)[O-])O[N+](=O)[O-]	38.0	7.5	11.9
2,3-dinitroxybutane	CC(O[N+](=O)[O-])C(O[N+](=O)[O-])C	105.5	36.5	11.7
1,4-dinitroxypentane	CC(CCCO[N+](=O)[O-])O[N+](=O)[O-]	9.24	7.9	12.2
1,5-dinitroxyhexane	CC(CCCCO[N+](=O)[O-])O[N+](=O)[O-]	5.2	6.8	12.5
2,5-dinitroxyhexane[c]	CC(CCC(C)O[N+](=O)[O-])O[N+](=O)[O-]	6.8	10.5	12.3
c-2,4-dinitroxypentane[c,d]	CC(CC(C)O[N+](=O)[O-])O[N+](=O)[O-]	27.8	13.3	11.9
t-2,4-dinitroxypentane[c,d]	CC(CC(C)O[N+](=O)[O-])O[N+](=O)[O-]	34.6	13.3	11.9
t-1,2-dinitroxycyclohexane[d]	C1(O-N(=O)O)CCCCC1O-N(=O)-O	5.6	6.6	12.4
c-1,2-dinitroxycyclohexane[d]	C1(O-N(=O)O)CCCCC1O-N(=O)-O	5.4	6.6	12.4
t-1,3-dinitroxycyclohexane[d]	O=[N+]([O-])OC1CCCC(O[N+](=O)[O-])C1	5.0	5.6	12.5
c-1,3-dinitroxycyclohexane[d]	O=[N+]([O-])OC1CCCC(O[N+](=O)[O-])C1	1.8	5.6	12.5
t-1,2-dinitroxycycloheptane[d]	C1(O-N(=O)O)CCCCCC1O-N(=O)-O	1.1	3.4	12.8

[a] F&B = Fischer and Ballschmiter (1998a, 1998b).
[b] Also see Section 4.4 and Figure 5.
[c] Also see Section 4.2 and Figure 3.
[d] We were unable to ascertain the difference in the molecular structures of molecules F&B distinguished with the labels "*c*-" and "*t*-" (see text for discussion).

4.4 Härtel et al. (2019)

Figure 5 compares the D-MPNN model's $P_{sat}(T)$ predictions for EGDN, NG, and 1,2,3,4-tetranitroxybutane to Härtel et al.'s (2019) measurement-based values. As found for the model's predictions for the molecules whose $P_{sat}(T)$ values were published by Kemp et al. (1957), the predictions were higher than the measurement-based values in the temperature range within which the measurements were performed. Moreover, the curvatures in the plots of the $P_{sat}(T)$ predictions were the opposite of what was expected. However, in the range of temperatures of particular interest (500–1000 K), the agreement was reasonable. Thus, the results were taken as further evidence supporting the use of the D-MPNN model for predicting MNGM's, DNGM's, and TNGM's $P_{sat}(T)$ values.

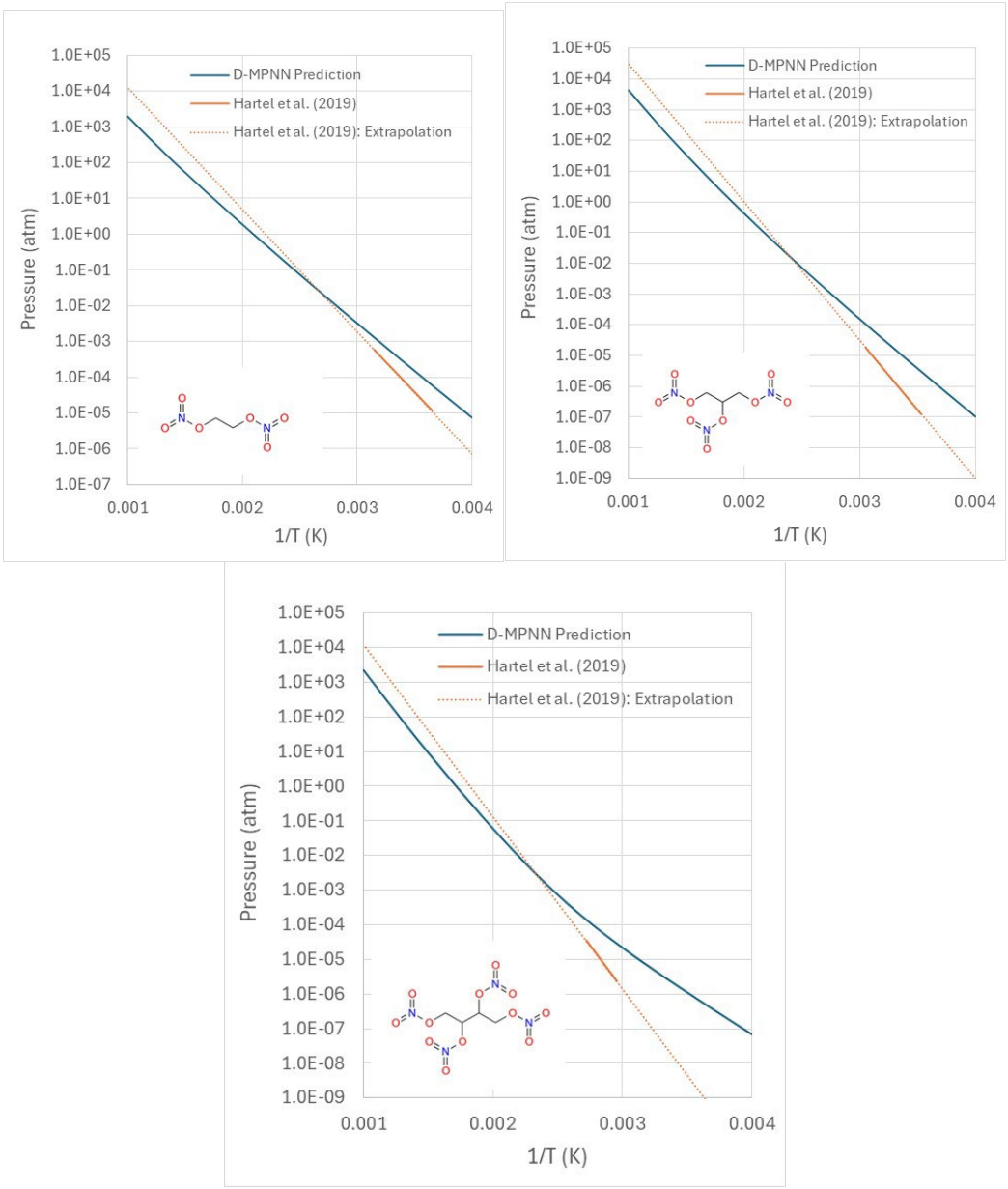

Figure 5. Comparison of predicted and measurement-based $P_{sat}(T)$ values for EGDN, NG, and 1,2,3,4-tetranitroxybutane.

5. $P_{sat}(T)$ Predictions for MNGM, DNGM, and TNGM

Figure 6 shows the D-MPNN model's $P_{sat}(T)$ predictions for MNGM, DNGM, and TNGM. It also shows the fits of Equation 4 to the predictions (with $C = 0$). The expressions corresponding to the fits were substituted into Equation 2 to produce the $\dot{m}_{l\to g}$ estimates presented in Section 6.

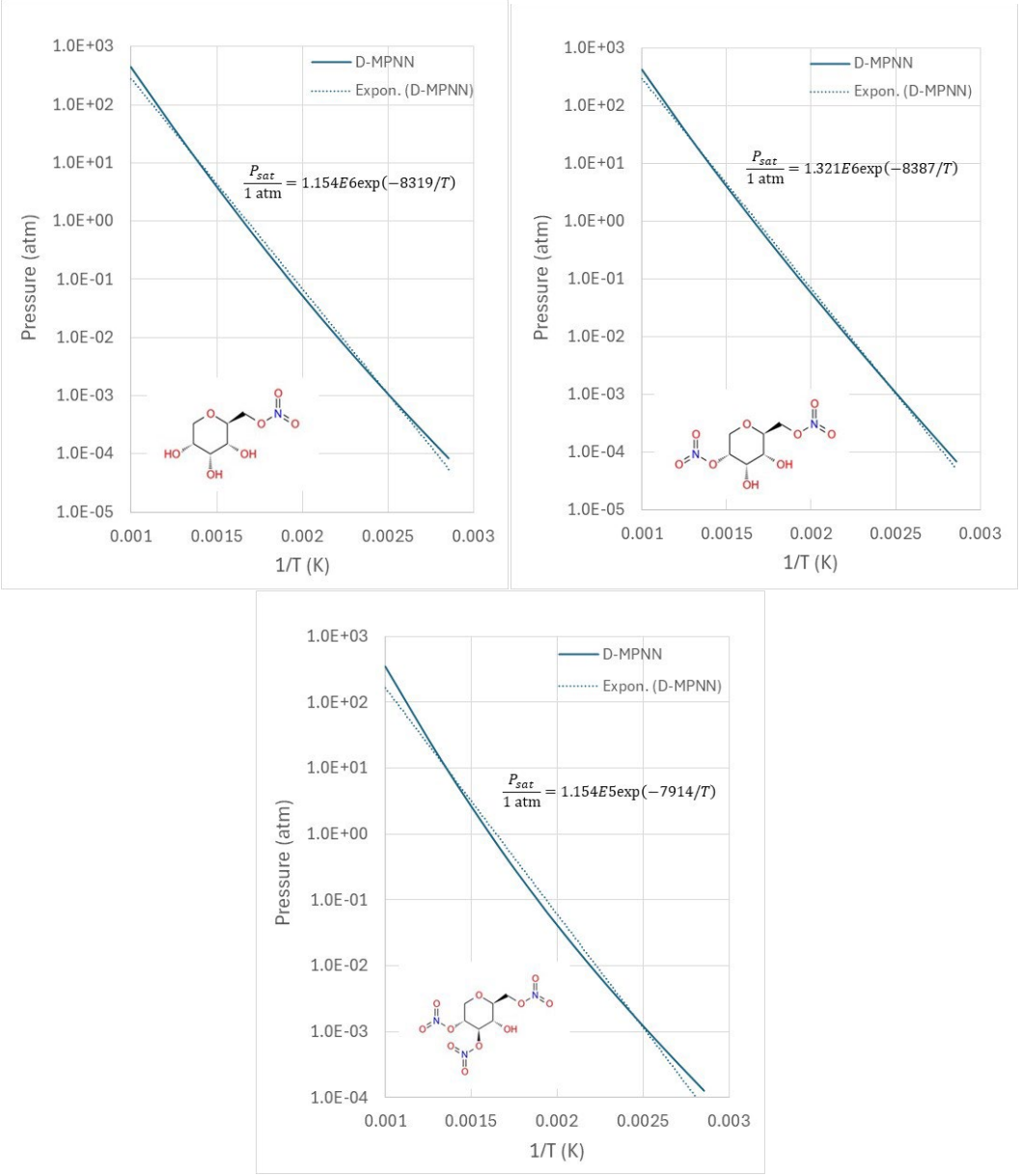

Figure 6. The D-MPNN model's $P_{sat}(T)$ predictions for MNGM, DNGM, and TNGM.

6. Comparison of Mass Flux Predictions from Pyrolysis Law and HLK Equations

Having observed that $P_{sat}(T)$ values in Equation 2 are generally well represented by formulae with the form $A\exp(-B/T)$, M.J.M. has long guessed that the general capacity of Equation 1 to well-represent measured $r(P)$ data derives from its correspondence to Equation 2. That is, in the limit $X_{k,g}^{+0} \to 0$, which (for example) obtains in the deflagration of ammonium perchlorate at high pressures (McQuaid and Chen 2014), the correspondence becomes almost one-to-one:

$$\dot{m}_{l\to g} = A'\exp\left(-\frac{B'}{T}\right) = c\sum_k \propto_k (W_k/2\pi RT^0)^{\frac{1}{2}}\left[X_{k,g}^{-0} A\exp\left(-\frac{B}{T}\right)\right], \qquad (6)$$

where c is a constant specified to bring the units of A' and $A\sum_k \propto_k (W_k/RT^0)^{1/2}$ into agreement. (The pre-exponential factor on the right side of Equation 6 includes a $(T^0)^{-1/2}$ dependence that A', which is a constant, does not have.) Therefore, we were curious how the $\dot{m}_{l\to g}$ values computed on the basis of HLK equations derived from the D-MPNN model's $P_{sat}(T)$ predictions for MNGM, DNGM, and TNGM would compare to those produced by Zenin's (1995) pyrolysis law for DBPs. The results are presented in Figure 7.

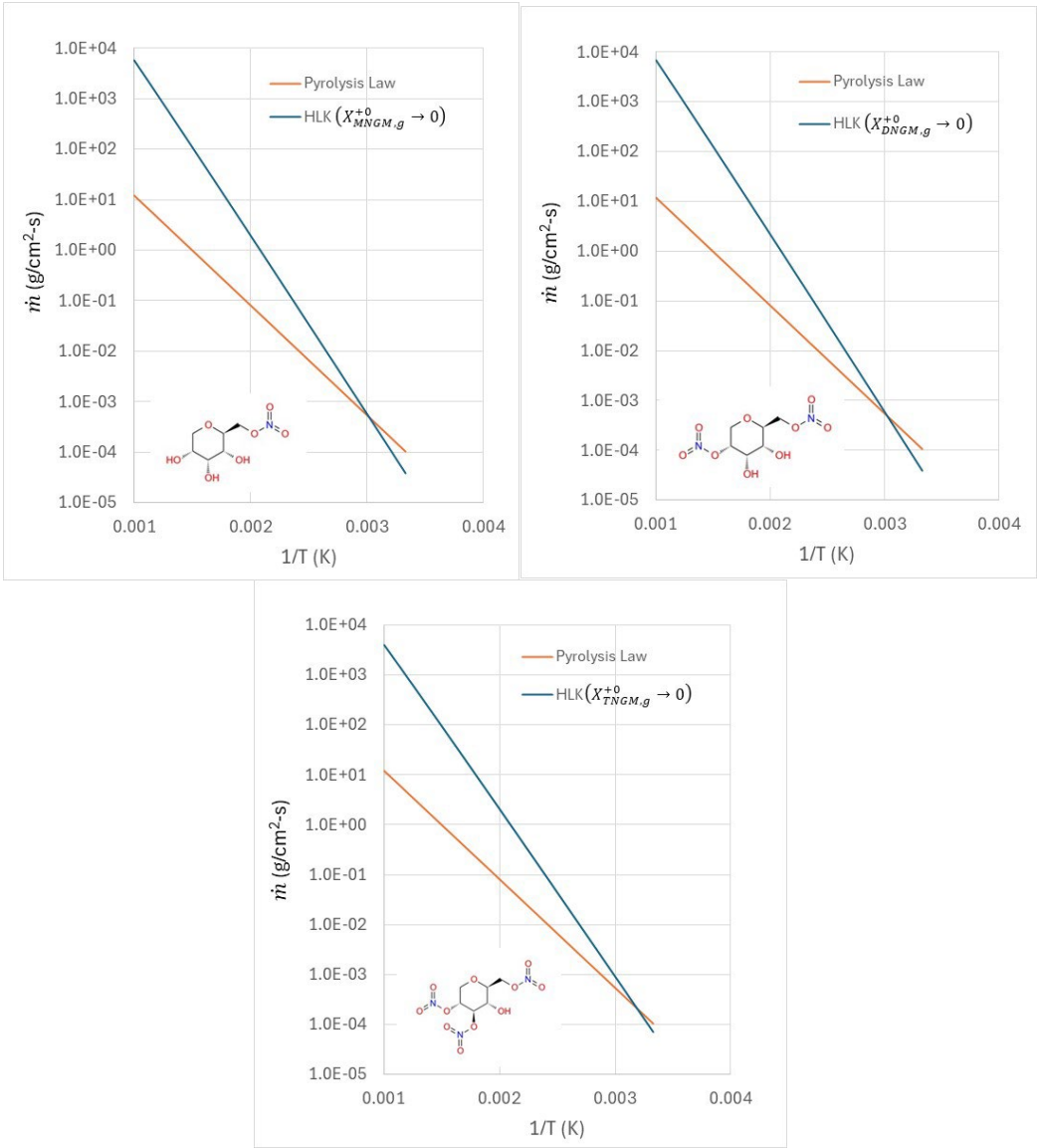

Figure 7. Comparison of $\dot{m}_{l\to g}$ predictions: Zenin's (1995) DBP pyrolysis law vs. the HLK equation in the limit $X_{k,g}^{+0} \to 0$.

As shown, for liquid-gas interface temperatures greater than approximately 333 K, the HLK equations (in the limit $X_{k,g}^{+0} \to 0$) generated $\dot{m}_{l\to g}$ estimates that were higher than those produced by Zenin's (1995) pyrolysis law (at a given T). However, at temperatures below 333 K, they generated lower $\dot{m}_{l\to g}$ estimates.

As mentioned in the introduction, NC does not readily decompose until temperatures exceed approximately 400 K, and presumably MNGM, DNGM, and TNGM will not either. Therefore, $X_{k,g}^{+0}$ values could well be significant relative to $X_{k,g}^{-0}$ in processes occurring in this temperature range, further reducing the $\dot{m}_{l\to g}$ estimates produced by the HLK equations. Coupling that expectation with the finding that Zenin's (1995) pyrolysis law overpredicted $\dot{m}_{l\to g}$ values at such temperatures (McQuaid et al. 2016), we believe that the HLK equations have the potential to generate better $\dot{m}_{l\to g}$ predictions for scenarios in which the dynamics of processes occurring at temperatures less than 400 K are important.

7. Summary and Conclusions

Toward creating HLK equations for physics-based models in which the molecules volatilizing from pyrolyzed NC are represented by MNGM, DNGM, and TNGM, we evaluated a D-MPNN model's predictions for the $P_{sat}(T)$ values of organic nitrate esters. Comparing predictions for 32 different alkyl nitrates to measurement-based values found in peer-reviewed papers, we observed reasonable agreement in most cases. Moreover, in cases where discrepancies were significant, they could be rationalized.

Based on those findings, we concluded that the model's $P_{sat}(T)$ predictions for MNGM, DNGM, and TNGM warranted use in formulating the desired HLK equations. Volatilization-rate predictions produced by those equations were compared to values produced by Zenin's (1995) pyrolysis law for DBPs. The results indicated that the HLK equations have the potential to produce better predictions for the rate at which pyrolyzed NC will volatilize at temperatures less than 400 K. Thus, they may find application in models for simulating the response of NC-containing EMs to thermal loads relevant to ignition and cook-off.

8. References

Anderson WR, Meagher NE, Vanderhoff JA. Dark zones of solid propellant flames: critically assessed datasets, quantitative model comparison, and detailed chemical analysis. Combust Flame. 2011;158:1228–1244.

Chen CC, Anderson WR, McQuaid MJ. Computationally based predictions for the burning rates and flame structures of nitroglycerin doped with various small molecules. CCDC Army Research Laboratory (US); 2019 June. Report No.: ARL-TR-8721.

Chen CC, Anderson WR, McQuaid MJ. Computationally based predictions for the burning rates and flame structures of nitroglycerin doped with various small molecules. Proceedings of the 41st JANNAF Propellant and Explosives Development and Characterization Subcommittee Meeting; 2018 Dec 10–13; Vancouver, WA.

Chen CC, McQuaid MJ. Thermochemical and kinetics studies of the pyrolysis of hydroxyl-terminated polybutadiene (HTPB). Proceedings of the 43rd JANNAF Combustion Subcommittee Meeting; 2009 Dec 7–11; La Jolla, CA.

Chen CC, McQuaid MJ. A detailed, gas-phase, finite-rate chemical kinetics mechanism for modeling the ignition and combustion of methyl and ethyl nitrate. Proceedings of the 60th JANNAF Propulsion Meeting; 2013 Apr 29–May 2; Colorado Springs, CO.

Chen CC, McQuaid MJ, Veals JD. Modeling the condensed-phase decomposition of nitrate esters. II: progress in developing a detailed finite-rate chemical kinetics mechanism for modeling the decomposition of nitrocellulose. Proceedings of the 43rd JANNAF Propellant and Explosives Development and Characterization Subcommittee Meeting; 2021a Dec 6–16; Virtual.

Chen CC, Veals JD, McQuaid MJ. Development and validation of detailed finite-rate chemical kinetics mechanisms for modeling the combustion of 1,3,5,7-tetranitro-1,3,5,7-tetrazocane-hydroxyl-terminated polybutadiene (HMX-HTPB) composites. DEVCOM Army Research Laboratory (US); 2021b May. Report No.: ARL-TR-9207.

Conner CB, Chen CC, Anderson WR. Chemical kinetics of solid propellant burning rate modifiers. Proceedings of the 42nd JANNAF Combustion Subcommittee Meeting; 2008 May 12–16; Boston, MA.

Fischer RG, Ballschmiter K. Prediction of the environmental distribution of alkyl dinitrates – chromatographic determination of vapor pressure p^0, water

solubility S_{H_2O}, gas-water partition coefficient K_{GW} (Henry's law constant), and octanol-water partition coefficient K_{OW}. Fresenius J Anal Chem. 1998a;360:769–776.

Fischer RG, Ballschmiter K. Determination of vapor pressure, water solubility, gas-water partition coefficient P_{gw}, Henry's law constant, and octanol-water partition coefficient P_{ow} of 26 alkyl dinitrates. Chemosphere. 1998b;36:2891–2901.

Gray P, Pratt MWT. The latent heats of vaporization of alkyl nitrates. J Chem Soc. 1957:2163–2168.

Härtel MA, Klapötke TM, Stierstorfer J, Zehetner L. Vapor pressure of linear nitrate esters determined by transpiration method in combination with VO-GC/MS. Propellants Explos Pyrotech. 2019;44:484–492.

Hsieh YL. Chemical structure and properties of cotton. Part I, Chapter 1. Cotton: Science and Technology; Woodhouse Publishing Series in Textiles; 2007 2007; p. 3–34.

Joback KG, Reid RC. Estimation of pure-component properties from group-contributions. Chem Eng Commun. 1987; 57: 233–243.

Jones DEG et al. The thermal decomposition of nitrocellulose. 34th International ICT-Conference; 2003 June 24–27; Karlsruhe, Germany.

Kemp MD, Goldhagen S, Zihlman FA. Vapor pressures and cryoscopic data for some aliphatic dinitroxy and trinitroxy compounds. J Phys Chem. 1957;61:240–242.

Lansford JL, Jensen KF, Barnes BC. Physics-informed transfer learning of out-of-sample vapor pressure predictions. Propellants Explos Pyrotech. 2023;48:e202200265.

Leider HR, Seaton DL. Nitrate ester decomposition and degradation of molecular weight in nitrocellulose from thermal decomposition of PBX-9404 below 100 C. Lawerence Livermore Laboratory (US); 1979 May. Report No.: UCRL-522776.

McQuaid MJ, Chen CC. Modeling the deflagration of ammonium perchlorate at pressures from 300 to 30000 psia. Part II: considerations besides the gas-phase, finite-rate chemical kinetics mechanism. Proceedings of the 46th JANNAF Combustion Subcommittee Meeting; 2014 Dec 8–11; Albuquerque, NM.

McQuaid MJ, Chen CC. A computationally based study of fizz zone effects on the linear burning rate of methyl nitrate. Proceedings of the 47th JANNAF Combustion Subcommittee Meeting; 2016a May 16–19; Newport News, VA.

McQuaid MJ, Chen CC. A computationally based study of the chemical suppression of AP-HTPB composite propellant burning rates. Proceedings of the 47th JANNAF Combustion Subcommittee Meeting; 2016b May 16–19; Newport News, VA.

McQuaid MJ, Chen CC, Stone CS, Veals JD. On modeling the pyrolysis of hydroxyl-terminated polybutadiene (HTPB) type R45M at temperatures in the range 465–600 °C. DEVCOM Army Research Laboratory (US); 2023 Apr 2023. Report No.: ARL-TR-9681.

McQuaid MJ, Chen CC, Veals J. Detailed gas-phase, finite-rate chemical kinetics mechanisms for slow cook-off response modeling: application in ARC test simulations. Presentation at: MSIAC Science of Slow Cook Off Workshop; 2016 Apr 25–29; Atlanta, GA.

McQuaid MJ, Chen CC, Veals JD. Simulating accelerating rate calorimetry experiments with a model having a detailed, gas-phase, finite-rate chemical kinetics mechanism: results for RDX. Proceedings of the 40th JANNAF Propellant and Explosives Development and Characterization Subcommittee (PEDCS) Meeting; 2017 May 22–25; Kansas City, MO.

McQuaid MJ, Chen CC, Veals J, Yeh IC. Detailed finite-rate chemical kinetics-based modeling of the decomposition of nitroglycerin in systems comprising liquid and gas phases. Proceedings of the 43rd JANNAF Propellant and Explosives Development and Characterization Subcommittee Meeting; 2021 Dec 6–16; Virtual.

Miller MS. Three-phase combustion modeling: frozen ozone, a prototype system. Army Research Laboratory (US); 1997 Mar. Report No.: ARL-TR-1320.

Miller MS, Anderson WR. Energetic-material combustion modeling with elementary gas-phase reactions: a practical approach. Prog Astronaut Aeronaut. 2000;185:501–531.

Miller MS, Anderson WR. Burning-rate predictor for multi-ingredient propellants: nitrate-ester propellants. J Propul Power. 2004;20:440–454.

Nusca MJ. Computational model of combustion in solid propellants with embedded metal wires. Proceedings of the 46th JANNAF Combustion Subcommittee Meeting; 2014 Dec 8–11; Albuquerque, NM. Chemical Propulsion Information Agency; CPIAC Publication JSC-CD-63.

Ostmark H, Wallin S, Ang HG. Vapor pressure of explosives: a critical review. Propellants Explos Pyrotech. 2012;37:12–23.

Saunders CW, Taylor LT. A review of the synthesis, chemistry and analysis of nitrocellulose. J Energ Mater. 1990;8:149–203.

Stone CP, Chen CC, Cornell R, McQuaid MJ. Simulating HTPB pyrolysis and combustion in an opposed-flow burner with detailed kinetics in a quasi-one-dimensional model. Spring Technical Meeting Eastern States Section of the Combustion Institute; 2024 Mar 10–13; Athens, GA.

Sućeska M, Musanic SM, Houra IF. Kinetics and enthalpy of nitroglycerin evaporation from double base propellants by isothermal thermography. Thermochim Acta. 2010;510:9–16.

Turcotte R et al. Thermal decomposition of nitrocellulose and its mixtures with nitroglycerine. 33rd International Pyrotechnics Seminar; 2006 July 16–21; Fort Collins, CO.

Veals JD, Chen CC, McQuaid MJ. Recent advances in modeling RDX combustion kinetics. Proceedings of the 49th JANNAF Combustion Subcommittee Meeting; 2019 June 3–7; Dayton, OH.

Veals JD et al. Property estimates for hydroxyl-terminated polybutadiene (HTPB) type R45M derived from atomistic molecular dynamics simulations. DEVCOM Army Research Laboratory (US); 2023 June. Report No.: ARL-TR-9714.

Zenin A. HMX and RDX: combustion mechanism and influence on modern double-base propellant combustion. J Propul Power. 1995;11:752–758.

Appendix. Implementation of the Joback Method for Estimating the Saturated Vapor Pressures of Organic Nitrate Esters

A simple and inexpensive means for estimating a wide variety of thermophysical and transport properties for (pure component) organic compounds is the well-known Joback group-contribution method.[1] Based on the assumption that the magnitudes of the interactions between functional groups that underlie the properties will be relatively independent of the molecule of which they are a member, it produces estimates by summing coefficients for the functional groups into which a molecule may be decomposed. Readily implemented via CheCalc,[2] the Joback method[1] can produce estimates for two properties that can be a basis for predicting a compound's/molecule's saturated vapor pressure (P_{sat}) as a function of temperature (T): its normal boiling point (T_{nbp}) and its enthalpy of vaporization at T_{nbp} [$\Delta H_v(T_{nbp})$]. They are estimated per

$$\frac{T_{nbp}}{1\ K} = 198.2 + \sum n_i c_{T_{nbp},i} \tag{A-1}$$

and

$$\frac{\Delta H_v(T_{nbp})}{1\ \mathrm{kJ/mol}} = 15.3 + \sum n_i c_{\Delta H_{vap},i}\,, \tag{A-2}$$

where n_i is the number of occurrences of each group (i) in the molecule and $c_{T_{nbp},i}$ and $c_{\Delta H_v,i}$ are coefficients that Joback and Reid[1] established for a wide variety of groups. The groups and their coefficients that are needed to estimate T_{nbp} and $\Delta H_v(T_{nbp})$ for the molecules considered in this study are shown in Table A-1.

Table A-1. Selected Joback[1] coefficients for estimating T_{nbp} and $\Delta H_v(T_{nbp})$.[2]

Substructures	$c_{T_{nbp}}$	$c_{\Delta H_v}$
non-ring groups		
-CH_3	23.58	2.373
-CH_2-	22.88	2.226
>CH-	21.74	1.691
ring groups		
-CH_2-	27.15	2.398
>CH-	21.78	1.942
oxygen groups		
-OH	98.88	16.826
-O- (non-ring)	22.23	2.410
-O- (ring)	31.22	4.682
nitrogen groups		
-NO_2	152.54	16.738

With respect to decomposing the molecules of interest into the functional groups in Table A-1, assignments were straightforward for all except the nitroxy groups

[1] Joback KG, Reid RC. Estimation of pure-component properties from group-contributions. Chem Eng Commun. 1987;57:233–243.
[2] CheGuide. Property estimation Joback method. CheGuide; c2025. https://cheguide.com/property_estimation.html

(−ONO_2). In their case, we recognized that (at a rudimentary level) their structure can be represented per −O−NO_2, and therefore we supposed that $c_{T_{nbp},-ONO_2}$ and $c_{\Delta H_v,-ONO_2}$ could be estimated per

$$c_{T_{nbp},-ONO_2} = c_{T_{nbp},-O-(non-ring)} + c_{T_{nbp},-NO_2} = 174.77 \qquad \text{(A-3)}$$

and

$$c_{\Delta H_v,-ONO_2} = c_{\Delta H_v,-O-(non-ring)} + c_{\Delta H_{vap},-NO_2} = 19.148. \qquad \text{(A-4)}$$

However, we presumed that Joback and Reid[1] derived $c_{T_{nbp},-O-(non-ring)}$ and $c_{\Delta H_v,-O-(non-ring)}$ based on T_{nbp} and $\Delta H_v(T_{nbp})$ values for molecules with C-O-C (ester) linkages and that $c_{T_{nbp},-NO_2}$ and $c_{\Delta H_v,-NO_2}$ were based on T_{nbp} and $\Delta H_v(T_{nbp})$ values for molecules with C-NO_2 groups. Therefore, we appreciated that the coefficients computed via Equations A-3 and A-4 might not produce reasonable T_{nbp} and $\Delta H_v(T_{nbp})$ estimates for nitrate esters.

Seeking a sense for the validity of estimates produced by Equations A-3 and A-4, we utilized them to estimate nitroglycerine's (NG's) T_{nbp} and $\Delta H_v(T_{nbp})$. The estimate for $\Delta H_v(T_{nbp})$ (27 kcal/mol) appeared to be somewhat high but not unreasonable. The estimate for T_{nbp} (790 K), however, appeared to be unreasonably high. (See the main body of the report for additional discussion of our bases for these conclusions.)

Having aggregated measurement-based $P_{sat}(T)$ data that could be used to estimate T_{nbp} and $\Delta H_v(T_{nbp})$ for a wide variety of alkyl nitrates, and therefrom $c_{T_{nbp},-ONO_2}$ and $c_{\Delta H_v,-ONO_2}$, we did so. Toward that objective, the Antoine equation

$$\log_{10}\left(\frac{P_{sat}}{1\ \text{atm}}\right) = A - \frac{B}{(T+C)}, \qquad \text{(A5)}$$

where A, B, and C are constants and T is the temperature in K, was fit to the $P_{sat}(T)$ data for alkyl nitrates that were published by Gray and Pratt,[3] Kemp et al.,[4] and Härtel et al.[5] Because the data from Kemp et al.[4] and Härtel et al.[5] fell within a relatively narrow temperature range, we did not believe that three-parameter fits to them were warranted, and therefore we set C equal to 0. Table A-2 shows the values of A, B, and C derived on these bases.

[3] Gray P, Pratt MWT. The latent heats of vaporization of alkyl nitrates. J Chem Soc. 1957:2163–2168.

[4] Kemp MD, Goldhagen S, Zihlman FA. Vapor pressures and cryoscopic data for some aliphatic dinitroxy and trinitroxy compounds. J Phys Chem. 1957;61:240–242.

[5] Härtel MA, Klapötke TM, Stierstorfer J, Zehetner L. Vapor pressure of linear nitrate esters determined by transpiration method in combination with VO-GC/MS. Propellants Explos Pyrotech. 2019;44:484–492.

Because $\log_{10}\left(\frac{P_{sat}(T_{nbp})}{1\ \text{atm}}\right)$ equals 0, it follows that

$$T_{nbp} = \frac{B}{A} - C. \tag{A6}$$

Further assuming that the Clausius–Clapeyron relationship between $P_{sat}(T)$ and $\Delta H_v(T)$ is valid for the molecules and temperature ranges considered, it can also be shown that

$$\Delta H_v(T_{nbp}) = \frac{2.303RBT_{nbp}^2}{(T_{nbp}+C)^2}. \tag{A-7}$$

Table A-2. Data used to derive $c_{T_{nbp},-ONO_2}$ and $c_{\Delta H_v,-ONO_2}$.[a]

	A	B K	C K	T_{nbp} K	$c_{T_{nbp}}$	ΔH_v kJ/mol	$c_{\Delta H_v}$
nitroxyethane[b]	4.2795	1337.04	-48.370	361	116.1	34	14.2
1-nitroxypropane[b]	4.8564	1721.72	-27.660	382	114.6	38	16.2
2-nitroxypropane[b]	3.5393	1018.57	-89.622	377	110.3	34	11.8
1-nitroxybutane[b]	5.4636	2177.07	-4.855	403	112.9	43	18.4
2-nitroxymethylpropane[b]	5.3196	2045.43	-8.996	394	103.5	41	17.0
1,3-dinitroxypropane[c]	8.5672	3880.00	0	453	93.0	74	26.2
1,3-dinitroxybutane[c]	8.1626	3726.68	0	457	83.6	71	23.8
1,4-dinitroxybutane[c]	5.3122	2997.93	0	564	137.3	57	16.6
1,5-dinitroxypentane[c]	8.7956	4104.08	0	467	77.0	79	26.1
2,4-dinitroxypentane[c]	6.3098	3139.51	0	498	92.9	60	17.2
1,2,4-trinitroxybutane[c]	4.8503	3131.69	0	646	119.0	60	12.1
NG I[c]	12.1119	5476.45	0	452	62.2	105	27.8
NG II[c]	13.0648	5745.71	0	440	58.0	110	29.5
EGDN[d]	7.5180	3411.90	0	454	104.9	65	22.8
NG[d]	9.0040	4501.90	0	500	78.1	86	21.6
1,2,3,4-tetranitroxybutane[d]	9.0570	4966.80	0	548	65.2	95	18.0
Average					[95.6]		[19.9]

[a] $\log_{10}(P_{sat}(T)/1\ \text{atm}) = A - (B/(T+C))$.

[b] Gray P, Pratt MWT. The latent heats of vaporization of alkyl nitrates. J Chem Soc. 1957:2163–2168.

[c] Kemp MD, Goldhagen S, Zihlman FA. Vapor pressures and cryoscopic data for some aliphatic dinitroxy and trinitroxy compounds. J Phys Chem. 1957;61:240–242.

[d] Härtel MA, Klapötke TM, Stierstorfer J, Zehetner L. Vapor pressure of linear nitrate esters determined by transpiration method in combination with VO-GC/MS. Propellants Explos Pyrotech. 2019;44:484–492.

Table A-2 shows for each molecule the T_{nbp} and $\Delta H_v(T_{nbp})$ estimates that were produced by Equations A-6 and A-7, respectively. The table also shows the $c_{T_{nbp},-ONO_2}$ and $c_{\Delta H_v,-ONO_2}$ values that were needed for the Joback method[1] to produce the T_{nbp} and $\Delta H_v(T_{nbp})$ estimates determined for each molecule. The average of the $c_{T_{nbp}}$ values was 95.6, which is similar to that for -OH groups (98.88) and considerably lower than the $c_{T_{nbp}}$ derived on the basis of Equation A-3.

The average of the $c_{\Delta H_v}$ values was 19.9, which was similar to the value found via Equation A4. We note that it is somewhat higher than the highest values in Table

A-1: 16.8 for -OH groups and 16.7 for -NO_2 groups. Given that ΔH_v values tend to increase with an increase in molecular size, we expected $c_{\Delta H_v,-ONO_2}$ to be greater than either $c_{\Delta H_v,-OH}$ or $c_{\Delta H_v,-NO_2}$.

Substituting $c_{T_{nbp},-ONO_2}$ = 95.6 and $c_{\Delta H_v,-ONO_2}$ = 19.9 into Equations A1 and A2, respectively, we obtained for NG T_{nbp} = 552.5 K and $\Delta H_v(T_{nbp})$ = 19.4 kcal/mol, both of which were more in line with our expectations. In addition, with these T_{nbp} and $\Delta H_v(T_{nbp})$ values substituted into Equation 3 of the main body of this report, the $P_{sat}(T)$ predictions shown in Figure A-1 were produced. Their overall agreement with both the directed-message passing neural network's (D-MPNN's) predictions and values published by Härtel et al.[5] suggest the reasonableness of the predictions. Therefore, we believe that with the addition of these coefficients, the Joback method[1] merits consideration for estimating T_{nbp} and $\Delta H_v(T_{nbp})$ for nitroxy-functionalized compounds if better alternatives cannot be identified or afforded.

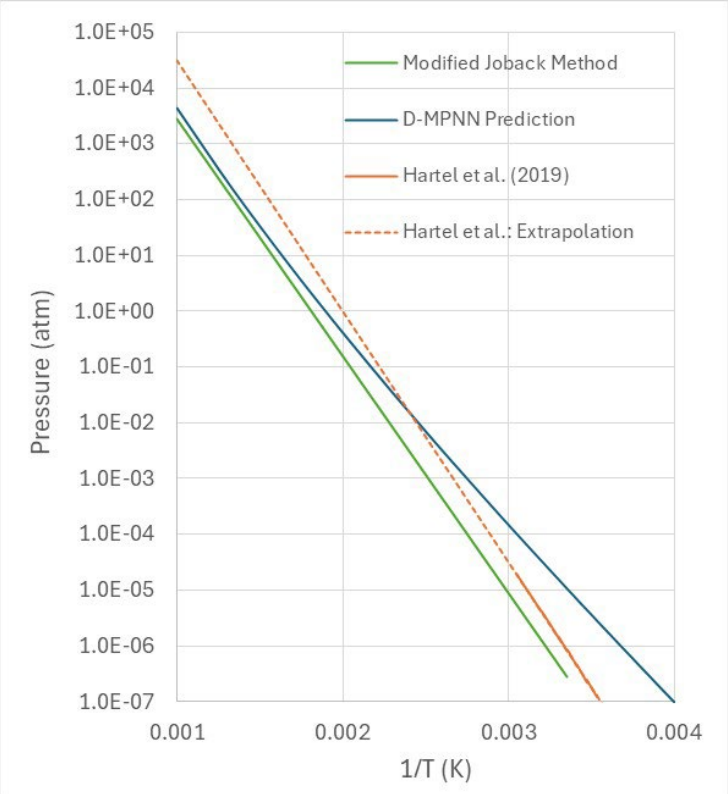

Figure A-1. Comparison of $P_{sat}(T)$ estimates for NG produced by various methods.

List of Symbols, Abbreviations, and Acronyms

DBP	double-base propellant
D-MPNN	directed-message passing neural network
DNB	dinitroxybutane
DNGM	[(3-nitroxy-4,5-dihydroxy) oxan-6-yl]methyl nitrate, ($C_6H_{10}N_2O_9$)
DZ	dark zone
EGDN	1,2-dinitroxyethane
EM	energetic material
EODT	6-ethenyl-2,8,12,16-octadectetraene ($C_{20}H_{32}$)
GM	anhydroglucose monomers
HLK	Hertz–Langmuir–Knudsen
HMX	1,3,5,7-tetranitro-1,3,5,7-tetrazocine
HTPB	hydroxyl-terminated polybutadiene
MNGM	[(3,4,5-trihydroxy)oxan-6-yl]methyl nitrate ($C_6H_{11}NO_7$)
MW	molecular weight
NC	nitrocellulose
NG	nitroglycerin
NPS	nascent product set
RDX	hexahydro-1,3,5-trinitro-1,3,5-triazine
RI	retention index
TNGM	[(3,4-dinitroxy-5-hydroxy)oxan-6-yl]methyl nitrate, ($C_6H_9N_3O_{11}$)
wt%	weight-percent

1 (PDF)	DEFENSE TECHNICAL INFORMATION CTR DTIC OCA
1 (PDF)	DEVCOM ARL FCDD RLB CI TECH LIB